



LAWRENCE
LIVERMORE
NATIONAL
LABORATORY

First-Generation Hybrid Compact Compton Imager

M. Cunningham, M. Burks, D. Chivers, C. Cork, L. Fabris, D. Gunter, T. Krings, D. Lange, E. Hull, L. Mihailescu, K. Nelson, T. Niedermayr, D. Protic, J. Valentine, K. Vetter, D. Wright

November 15, 2005

IEEE Nuclear Science Symposium
Fajardo, PR, United States
October 23, 2005 through October 29, 2005

Disclaimer

This document was prepared as an account of work sponsored by an agency of the United States Government. Neither the United States Government nor the University of California nor any of their employees, makes any warranty, express or implied, or assumes any legal liability or responsibility for the accuracy, completeness, or usefulness of any information, apparatus, product, or process disclosed, or represents that its use would not infringe privately owned rights. Reference herein to any specific commercial product, process, or service by trade name, trademark, manufacturer, or otherwise, does not necessarily constitute or imply its endorsement, recommendation, or favoring by the United States Government or the University of California. The views and opinions of authors expressed herein do not necessarily state or reflect those of the United States Government or the University of California, and shall not be used for advertising or product endorsement purposes.

First-Generation Hybrid Compact Compton Imager

Mark Cunningham^a, Morgan Burks^a, Dan Chivers^b, Chris Cork^a, Lorenzo Fabris^a, Donald Gunter^a, Thomas Krings^c, David Lange^a, Ethan Hull^a, Lucian Mihailescu^a, Karl Nelson^a, Thomas Niedermayr^a, Davor Protic^c, John Valentine^a, Kai Vetter^a, and Doug Wright^a

Abstract—At Lawrence Livermore National Laboratory, we are pursuing the development of a gamma-ray imaging system using the Compton effect. We have built our first generation hybrid Compton imaging system, and we have conducted initial calibration and image measurements using this system. In this paper, we present the details of the hybrid Compton imaging system and initial calibration and image measurements.

I. INTRODUCTION

Compton imagers are a promising technology for efficiently and precisely imaging sources of gamma rays. Applications include astrophysics, medical imaging and Homeland Security operations. These imaging systems require that a gamma-ray first Compton scatter and then subsequently interact at least once more within the active volume of the imager. For an unknown spectrum of gamma rays, Compton imaging further requires that the detector records both the positions of the first two interactions and the energy deposited by the first Compton scatter interaction, and measures the incoming gamma-ray energy. The origin of the incident gamma ray can then be confined to a conical surface whose axis is determined by the interaction locations, apex is determined by the first interaction location, and half-angle is given by the Compton scatter equation[1]. An image of a radioactive source is constructed by projecting these cone surfaces on a two-dimensional surface. The location of a particular radioisotope is identified by the overlapping rings of the energy bands associated with the emission lines of the radioisotopes[2].

As a long-term goal, we plan to construct Compton imagers that are capable of detecting, identifying and localizing a radioisotope of interest in the presence of a non-localized, non-uniform distribution of background radioactive sources for a range of applications. We have built a first-generation hybrid prototype to work towards this goal. The intention of this first prototype is multifold: Address the engineering challenges associated with building deployable Compton imagers; establish pulse-shape analysis techniques required to extract the positions and energies of a maximum number of interactions; develop the data analysis algorithms necessary to maximize the number of correctly reconstructed interaction sequences; and benchmark the system with Monte Carlo simulations in order to both improve the design and enable the prediction of the performance of future imaging systems.

In this paper we present the details of our first-generation prototype. Specifically, we describe the details of the

detectors, data acquisition system, and the initial calibration and image measurements.

II. COMPTON IMAGING SYSTEM

The overall concept of our effort is to develop an integrated and deployable gamma-ray imaging system that can detect, identify, and localize a threat source in the energy range of ~120 keV to 3000 keV and in real time. The term integrated refers to the assembly of multiple gamma-ray sensors in a single cryostat, the coupling of the electronic signals from the strips on these sensors to the pre-amplifiers, the conversion of the pre-amplifier output from an analog signal to a digital signal, and the processing of these digital signals to display a gamma-ray image of the radioactive environment in a single gamma-ray imaging system. The term deployable refers to the ability to put the gamma-ray imager in a strategically important location for surveillance; therefore, the system must be designed with a particular scenario in mind. For this first prototype imaging system, we define deployable as the ability to move the system within a laboratory environment.

Our approach to building an integrated and deployable system is to design and assemble a series of prototype systems. We will leverage the knowledge acquired from building each previous prototype to build a more sophisticated system in incremental steps. This approach enables us to avoid the large engineering risks inherent in attempting to build the final system from the beginning of the project. At present, we have built the first prototype system (CCI1), imaged radioactive sources, and initiated the benchmarking process. In addition, we are in the process of building the second prototype system (CCI2).

In order to build our first prototype hybrid Compton imaging system, we chose to build on our experience of assembling single crystals inside a cryostat; therefore, we assembled a germanium crystal in one cryostat and a silicon crystal in another cryostat. A picture of the single Ge sensor inside a cryostat is shown in Fig. 1. The germanium crystal is patterned with orthogonal strips on opposite sides of the crystal. The high voltage electronics and infrared shield surrounding the crystal are contained within the cryostat. Individual wires connect each strip on the crystal to a pre-amplifier outside the vacuum vessel containing the germanium crystal. The two cryostats, one with a silicon crystal and one with a germanium crystal, are mounted on top of a mobile platform. This mobile platform, shown in Fig. 2-3, includes: pre-amplifiers, post-amplifiers, NIM modules, ADCs, and a computer with data acquisition and processing software.

^a Lawrence Livermore National Laboratory, U.S.A.

^b University of California, Berkeley, U.S.A.

^c Forschungszentrum Jülich GmbH, Institut für Kernphysik, 52425 Jülich, German.

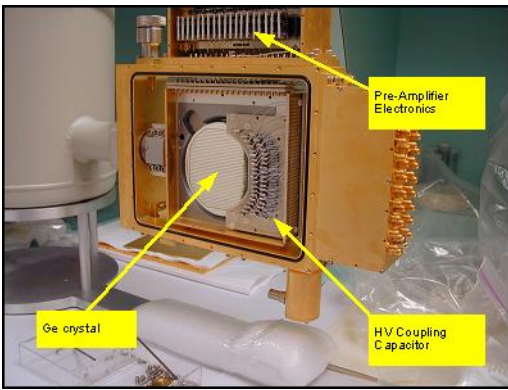


Fig. 1: Our conventional single Ge gamma-ray crystal cryostat.

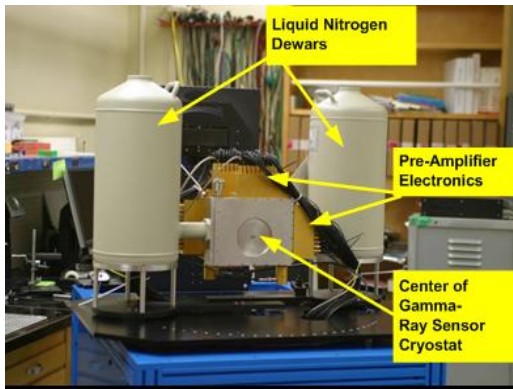


Fig. 2: View of the cryostats on the mobile Compton imaging platform.



Fig. 3: The integrated mobile hybrid Compton imaging platform.

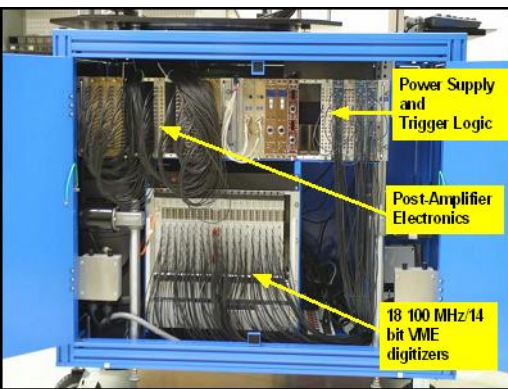


Fig. 4: View of electronics for the mobile Compton imaging platform.

The Ge crystal is made from high-purity germanium (HPGe) with an impurity concentration of about $5 \times 10^9 \text{ cm}^{-3}$.

There are 38 strips on each side of the crystal, and the strips on opposite sides are implemented in an orthogonal geometry. The pitch of the strips is 2 mm, and the gap between strips is 0.25 mm. The sensitive volume of the germanium detector has a diameter of 76 mm and a thickness of 11 mm. The contacts and passivation of the Ge crystal are made with amorphous Ge[3]. The segmentation structure was implemented by evaporating aluminum through a mask. Only the metallization of the Ge contact defines the segmentation structure, including the guard ring. The underlying amorphous Ge contact is kept intact. The depletion voltage of this detector is $\sim 400 \text{ V}$ and it is operated at 1000 V. This crystal was fabricated at LLNL by Ethan Hull.

The Si crystal is made from a 10 cm Si wafer and has a thickness of 10 mm. The crystal was cut into a square shape to provide equal strip lengths. The active area is $64 \times 64 \text{ mm}^2$ with a 10 mm wide guard ring. The silicon crystal has 32 strips on each side of the crystal, and the strips on opposite sides are orthogonal. The pitch of the strips is 2 mm, and the gap between strips is 0.05 mm. Despite its low impurity concentration, the detector needs to be operated at 2000 V. This high operating voltage is probably due to the insufficient Li drift in three of the middle strips. The blocking contacts for Si(Li) are made with Lithium and Boron. An etching step is used to slightly etch into the crystal to reduce capacitive coupling between the strips. This silicon crystal was fabricated by Davor Protic of the Research Center in Juelich Germany.

There are two-stages of amplification in this system. The pre-amplification is based on a previously demonstrated compact low-noise, low-cost design[4]. The preamplifier stage is constructed around a high-open loop gain N-channel FET. The input capacitance of this device is comparable to the input capacitance of the detector strips. The second stage is AC-coupled to the preamplifier through a $50 \mu\text{s}$ time constant. This application-tailored coupling provides a convenient decay time constant to couple the analog circuit to the digital back-end. The second stage is capable of driving a 50Ω impedance cable terminated at the back-end. The total power consumption for each channel is $\sim 120 \text{ mW}$.

The signal output of the amplification stages is connected via coaxial cables to an 8-channel DAQ module. These modules are commercially available from Struck Innovative Systems (SIS). Each module contains 8 analog-to-digital converters, a set of FPGA devices to post process each channel, a dedicated memory buffer for each FPGA, and a FPGA to handle both triggering and VME bus interactions. These DAQ modules are contained in a VME crate containing a single VME-to-PCI converter (SIS3100/SIS1100). The ADC boards (SIS3301) have a resolution of 14 bit and are operated at a sampling rate of 100 MHz. Data is transmitted via an optical cable from the VME crate to a PCI board in a DAQ computer. Contained in the VME-PCI converter board is a DSP on a piggy backed SIS9200 card. Each module also produces a trigger output that is combined and propagated back to each module to establish a common readout.

All modules are synchronized with an external clock, which is distributed through coaxial cables. All channels of each side

of both the Si and Ge sensors are processed by four and five ADC boards, respectively; therefore, we operate 18 ADC boards simultaneously. Each channel is able to generate an external, local trigger output signal for each board. These external trigger signals are combined logically in NIM modules to define a global trigger; therefore, this system can be used to trigger on coincidence events or each detector independently. The global trigger signal is then distributed back to the individual boards to initiate the readout.

III. CALIBRATION AND INITIAL MEASUREMENTS

The initial measurements with CCI1 were conducted to calibrate each sensor for both energy and depth of interaction inside the crystals. In order to do an energy calibration of both the Ge and Si, an Am241 gamma-ray source was used for a low energy calibration point and a Cs137 gamma-ray source was used for a high energy calibration point. The resolution of each strip of both the Ge and the Si for both 60 keV and 662 keV is shown in Fig. 5-8. The two sides of both the Ge and Si crystals are labeled either AC or DC corresponding to the method of coupling between each strip on the crystal and the associated pre-amplifier. Strips 4-6 on the AC side of the Si crystal are not shown in Fig. 5-6. High leakage current in these strips prevented the high-resolution operation of these strips at the required operating voltage. As can be seen, the strips close to these strips also show degraded energy resolution due to high leakage current. In addition, at 662 keV, all strips from this side display a degradation in energy resolution.

The z-depth calibration of both the Ge and Si crystals was measured by placing an Am241 source first on the AC side of each crystal and then on the DC side of each crystal. The time difference of the arrival time between the AC-side signal and the DC-side signal for Ge is shown in Fig. 9. A Gaussian curve was fit to the outside portion of each peak to estimate the timing resolution of the system. Using the time difference between the peaks and assuming a linear fit, we can determine the depth of interaction of a gamma-ray event. In this way, we obtain a depth resolution (FWHM) at 60 keV of 1.8 mm and 1.1 mm for Si and Ge, respectively.

Gamma-ray imaging measurements have also been made with our hybrid Compton imaging system, as shown in Fig. 10. This image was taken with the source in the horizontal plane and 30 degrees off the detector axis. The source for this image was Eu152. The image in Fig. 10 is made with the 1408 keV photopeak. The x and y axis represent theta and phi respectively (in degrees). The vertical axis is proportional to the intensity. The image was made with back-projection of the Compton rings. No image reconstruction was done.

More details concerning the imaging resolution of this system is given elsewhere in the conference proceedings. See paper by Morgan Burks et al.

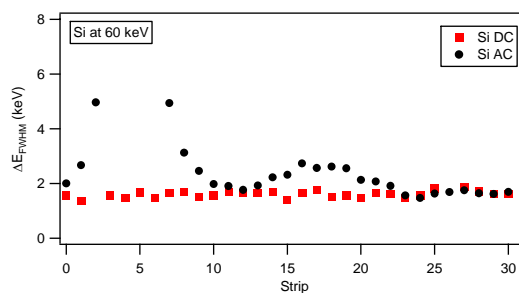


Fig. 5: Energy Resolution for Si at 60 keV

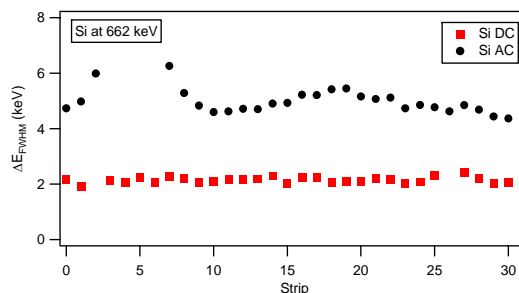


Fig. 6: Energy Resolution for Si at 662 keV.

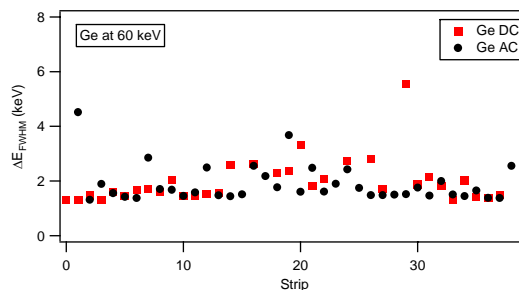


Fig. 7: Energy Resolution for Ge at 60 keV.

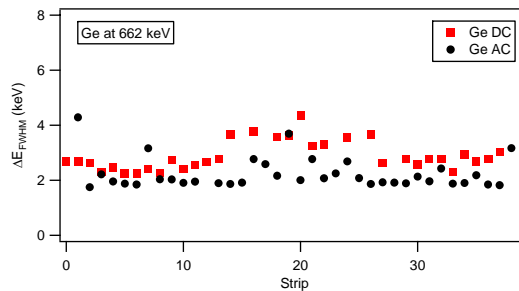


Fig. 8: Energy Resolution for Ge at 662 keV.

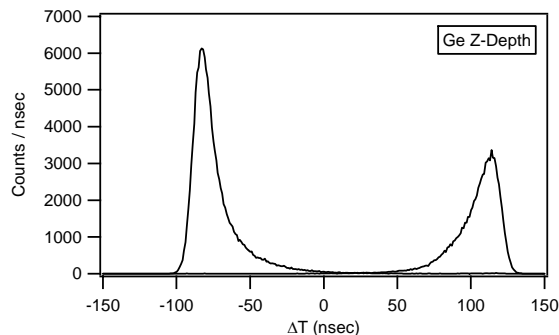


Fig. 9: Arrival time difference between the AC-side signal and the DC-side signal.

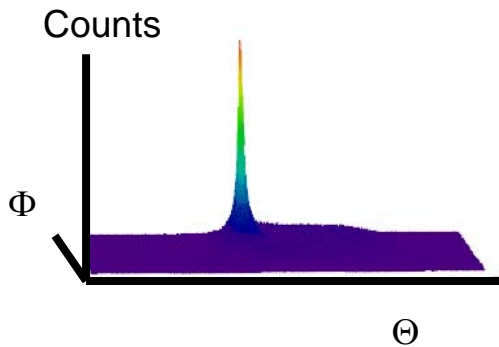


Fig. 10: 4π Field of View image.

IV. CONCLUSION

At Lawrence Livermore National Laboratory, we are pursuing the development of a gamma-ray imaging system using the Compton effect. We have built our first generation hybrid Compton imaging system, and we have conducted initial calibration and image measurements using this system. In this paper, we have presented the details of the detectors and data acquisition system of the hybrid Compton imaging system and the initial calibration and image measurements.

ACKNOWLEDGMENT

This work was performed under the auspices of the U.S. Department of Energy by University of California, Lawrence Livermore National Laboratory under Contract W-7405-Eng-48.

REFERENCES

- [1] Glenn Knoll, *Radiation Detection and Measurement*, 3rd ed. John Wiley & Sons, Inc., 2000.
- [2] Miles Wernick and John Aarsvold, *Emission Tomograph*. Elsevier Academic Press, 2004.
- [3] M. Amman and P. N. Luke, "Three-Dimensional Position Sensing and Field Shaping in Orthogonal-Strip Germanium Gamma-Ray Detectors," *MINA*, pp. 155-166, 2000.
- [4] L. Fabris, N. W. Madden and H. Yaver, "A fast, compact solution for low noise charge preamplifiers," *NIM A*, vol 424, Is. 2-3, pp. 545-551, March 1999.